

## Article

# Preconcentration of a Medium-Grade Celestine Ore by Dense Medium Cyclone Using a Factorial Design

Noemi Ariza-Rodríguez <sup>1,2</sup> , Alejandro B. Rodríguez-Navarro <sup>3,\*</sup>, Francisco Ortega <sup>1,2</sup>, Mónica Calero de Hoces <sup>1</sup> and Mario J. Muñoz-Batista <sup>1,\*</sup> 

<sup>1</sup> Departamento de Ingeniería Química, Universidad de Granada, 18002 Granada, Spain; noemiar@correo.ugr.es (N.A.-R.); francisortega@correo.ugr.es (F.O.); mcaleroh@ugr.es (M.C.d.H.)

<sup>2</sup> Canteras Industriales S.L., 18110 Las Gabias, Granada, Spain

<sup>3</sup> Departamento de Mineralogía y Petrología, Universidad de Granada, 18002 Granada, Spain

\* Correspondence: anava@ugr.es (A.B.R.-N.); mariomunoz@ugr.es (M.J.M.-B.)

**Abstract:** A semi-industrial scale hydrocyclone with a 250 mm internal diameter was used to concentrate medium-grade celestine ore (75%–85% celestine) from the Montevive deposit of Granada (Spain) using a dense ferrosilicon (FeSi) medium. For this purpose, a Box–Behnken factorial design (BBD) was carried out, with the response variable being the Sr concentration measured by X-ray fluorescence (XRF), as well as the concentration of celestine measured by X-ray diffraction (XRD) of the mineral collected from the under (sunk) stream of the hydrocyclone. The experimental factors to be optimised were the density of the medium in the mixing tank (water, FeSi, and feed mineral) varying from 2.7 to 2.9 kg/L, the hydrocyclone inlet pressure from 0.8 to 1.2 bar, and the hydrocyclone inclination (from 15° to 25° from the horizontal). The range of densities of the dense medium to be tested was determined from previous sink–float experiments using medium-grade ore, in which the distribution of mineral phases with different particle size fractions was determined. To evaluate the separation behaviour, the following parameters were considered: the enrichment ratio (E), the tailings discarding ratio (R), and the mineral processing recovery ( $\epsilon$ ). From the factorial design and the response surface, the optimum parameters maximising celestine concentration in the under stream (78%), were determined. These optimised parameters were: a density of 2.75 kg/L for the dense medium, an inlet pressure of 1.05 bar, and a hydrocyclone inclination varying from 18° to 20°. Under these conditions, a 94% recovery of celestine (68% Sr) can be achieved. These results show that medium-grade celestine ore, accumulated in mine tailings dumps, can be effectively concentrated using DMS hydrocyclones and that the operating parameters can be optimised using a factorial experiment design. This study can contribute to reducing overexploitation of strategic mineral resources, avoiding blasting and environmentally damaging clearing, by applying a simple and sustainable technique.



**Citation:** Ariza-Rodríguez, N.; Rodríguez-Navarro, A.B.; Ortega, F.; Calero de Hoces, M.; Muñoz-Batista, M.J. Preconcentration of a Medium-Grade Celestine Ore by Dense Medium Cyclone Using a Factorial Design. *Minerals* **2024**, *14*, 306. <https://doi.org/10.3390/min14030306>

Academic Editor: Carlos Hoffmann Sampaio

Received: 15 January 2024

Revised: 8 March 2024

Accepted: 12 March 2024

Published: 14 March 2024



**Copyright:** © 2024 by the authors. Licensee MDPI, Basel, Switzerland. This article is an open access article distributed under the terms and conditions of the Creative Commons Attribution (CC BY) license (<https://creativecommons.org/licenses/by/4.0/>).

**Keywords:** celestine; DMS method; hydrocyclone; Box–Behnken; factorial design

## 1. Introduction

Our society's demand for raw materials and minerals is constantly increasing as new technological applications are found, and greater volumes are needed for our industry. The increase in production requires adequate waste and water management policies in mining operations to be sustainable while preventing irreparable damage to the environment.

Strontium was included in 2021 as one of the 30 critical raw materials (CRMs) for the European Union [1], with the largest reserve in Europe placed in the Montevive mine. In Montevive, celestine ore (the main source of strontium) is exploited in the Aurora Mine (Mining Group No. 99012) as an open pit [2]. The exploitation covers an area of 332 Ha or 11 mining grids.

The mine produces over 100,000 tons of medium-high-grade minerals (80%) per year. High-grade celestine ore has traditionally been sorted manually, generating a large amount

of uneconomical low-medium ore (60%–80%) that has been accumulated in the mine tailings [3]. At present, the processing of medium-low-grade ore is based on traditional mining activities (crushing, grinding, sorting, grading, conveying, and loading). It is therefore essential to adopt newer and more advanced mining methods that allow the concentration of the low-medium celestine ore. At the same time, it is necessary to use methods that minimise water and energy use. In this sense, different solutions are currently proposed, such as using ore pre-concentration methods to eliminate tailings and using more energy-efficient methods (as well as cost-effective and environmentally friendly) [4–6].

The methods used for the concentration of strontium ores are several and diverse, but all of them aim to separate the ore or mineral of economic interest from the gangue. For this purpose, different equipment and methodologies are applied based on differences between the ore and gangue minerals in particle size (classification); differences in density (gravimetric concentration) [7]; or differences in surface properties of the different mineral species (flotation) [8–10] (-).

Previous studies have demonstrated that gravity separation techniques are very suitable for the beneficiation of low-grade celestine mineral (about 70% celestine), which is currently uneconomical and accumulated in dumps and mine tailings. This mineral can be concentrated based on mineral separation and classification after grinding and celestine concentration by dense medium separation methods (DMSs) [3,11]. The proposed method for celestine ore concentration is based on the difference in density between the mineral phase of interest (celestine) and the rest of the uneconomical mineral phases (gravimetric concentration). Density-based separation technologies have historically been used to process a variety of materials [12]. In particular, dense media cyclones (DMCs) have been widely used in mineral processing due to their advantages, including large processing capacity, high separation efficiency, and easy automatic control [13].

This equipment is used in the separation of particles in the range of 150  $\mu\text{m}$  to 0.5 mm in a dense medium. The dense medium is a suspension in water of fine particles of typically magnetite, ferrosilicon, or ilmenite, with concentrations that depend on the densities of the ore and gangue minerals. For the operation, hydrocyclone (Supplementary Material) are tilted an inclination angle between 10–15° with respect to the horizontal to avoid displacement of the dense medium by gravitational force.

The dense media (ferrosilicon, magnetite, or ilmenite) with the ore particles are fed into the hydrocyclone tangentially, creating a vortex. Thus, the mineral particles are subjected to two opposing forces: a centrifugal force that pushes the dense particles (in this case, celestine) to migrate towards the wall and a drag force that causes the light particles (gangue mineral such as calcite) to move towards the central axis [13].

In this study, we have used a semi-industrial scale hydrocyclone to concentrate medium-grade celestine ore (75%–85% celestine) from the Montevive deposit of Granada (Spain) using a dense ferrosilicon (FeSi) medium. A Box–Behnken factorial design (BBD) was used to determine the optimum conditions to concentrate the celestine mineral, using the celestine concentration as the response and the density of the medium, the hydrocyclone inlet pressure, and the hydrocyclone inclination angle as experimental operational factors. This study can contribute to making the mineral exploitation of Montevive more sustainable by using waste mineral from the mine dumps and tailings while avoiding new blasting and clearing, which are environmentally damaging.

## 2. Materials and Methods

### 2.1. Montevive Celestine Mineral

For the float–sink tests, 15 kg of celestine ore with a medium grade (83.33% celestine) and a particle size ranging from 0.1 to 10 mm were used (see Tables 1 and 2 and Figure 1). A sample of 10 tons of medium-grade celestine ore (77.23% celestine) from Montevive's tailings was recovered for validation tests in the hydrocyclone (Tables 1 and 2, Figures S1 and S2). The chemical and mineralogical composition of the mineral was determined by X-ray diffraction (XRD) using a Xpert Pro X-ray powder diffractometer (Pana-

lytical, Almelo, The Netherlands). The samples were measured in reflection mode using copper radiation (from 4 to 120° with 0.017° step size and 100 s integration time per step). Identification of the main mineral phases present in the samples was carried out using XpolderX software (version 2021.04.21). For quantitative mineral analyses, XRD patterns were analysed using the Rietveld refinement method with Topas v 5.0 software (Bruker, Billerica, MA, USA). The main XRD results are summarised in Table 1 and show that celestine (83.33% in the float–sink sample; 77.23% in the validation sample) and calcite (9.79% in the float–sink sample; 12.89% in the validation sample) were the main mineral phases detected in the float–sink tests. Other minority mineral phases (<10%) were strontianite, quartz, dolomite, and illite. Additionally, the chemical composition of samples was analysed by X-ray fluorescence (XRF) using an S2 Ranger Bruker energy-dispersive spectrometer (Bruker-AXS, Karlsruhe, Germany) equipped with an X-ray tube with Pd anode and an EDX detector with <155 eV resolution. The system was calibrated using a Cu disk and checked with a glass BAXS-S2. The main results obtained by XRF are summarised in Table 2.

In the case of the hydrocyclone validation sample, the predominant mineral phases were also celestine and calcite, as deduced from the XRD and XRF data.

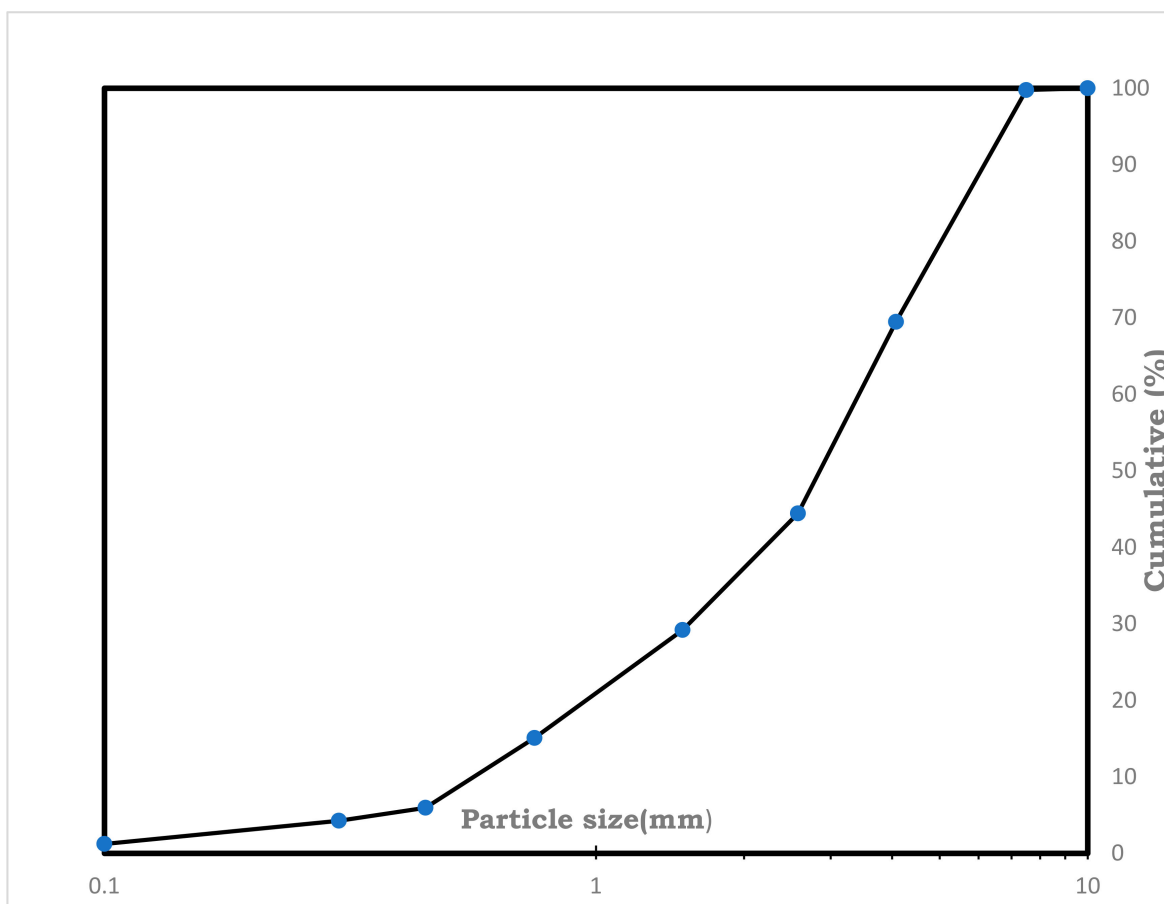


Figure 1. The cumulative particle size distribution of celestine ore samples.

Table 1. Summary of chemical composition of celestine ore samples determined by XRF.

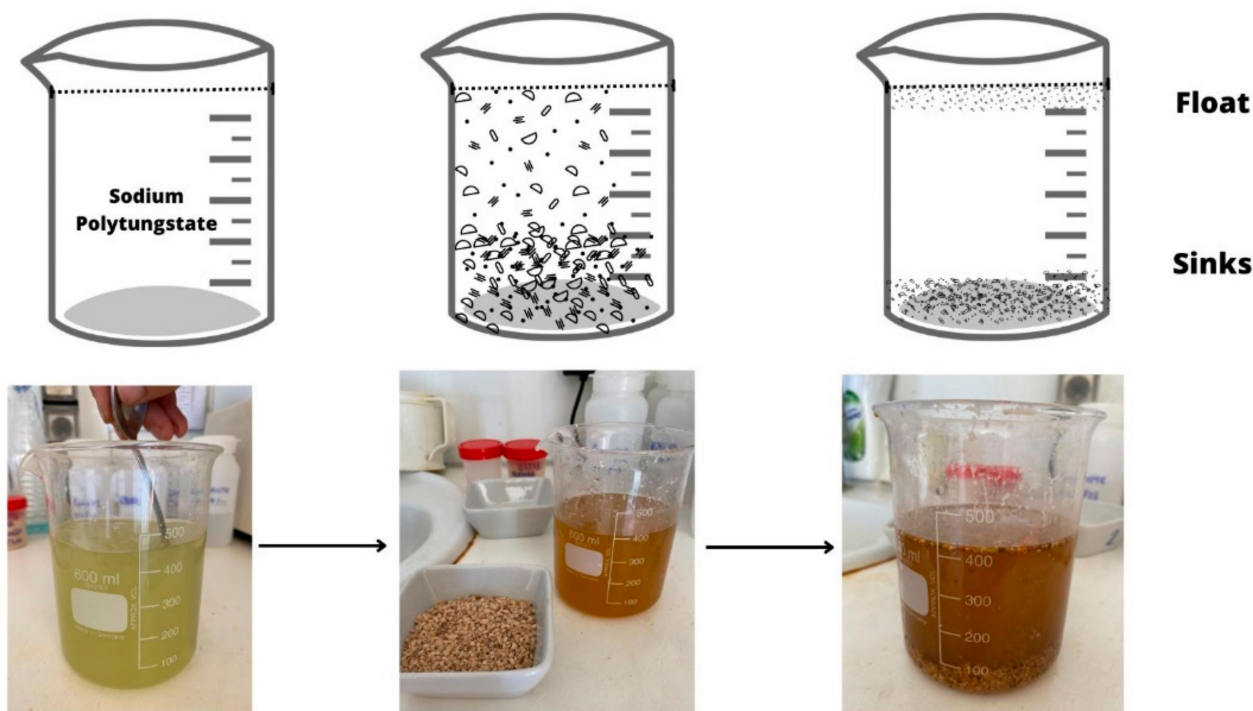
	Sr (%)	Ba (%)	Fe (%)	Si (%)	Mg (%)	Ca (%)
Float–sink test	60.08	2.27	1.52	4.55	1.20	18.39
Validation test (Figure S2)	54.75	1.80	2.70	1.80	1.54	16.66

**Table 2.** Summary of mineral composition of celestine ore samples determined by XRD.

	Celestine (%)	Strontianite (%)	Quartz (%)	Dolomite (%)	Calcite (%)	Illite (%)
Float–sink test	83.33	0.40	3.39	2.54	9.79	0.55
Validation test (Figure S2)	77.23	0.00	2.45	4.88	12.89	2.55

## 2.2. Float–Sink Tests

To determine the optimum density of the dense medium for the separation experiments, a set of float–sink tests was carried out using the DMS hydrocyclone. Sodium polytungstate (SPT-1; SG: 3.10; Sometu Europa, CAS-No:12141-67-1) was diluted at different concentrations in water to prepare the dense medium with different densities (2.7, 2.8, 2.9 kg/L). Then, the ore mineral was classified into fractions with different particle sizes using a vibrating screen (>5 mm; –5 mm + 3.15 mm; –3.15 mm + 2 mm; –2 mm + 1 mm; <1 mm). Next, the mineral fraction with a given particle size (100 g) was mixed in the dense medium and then left to sit (Figure 2). Then, the mineral separated into the float and sunk fractions were recovered, washed with Milli-Q water, and dried in an oven at 120 °C for 24 h.

**Figure 2.** Float–sink test.

The mineral was ground below 60  $\mu\text{m}$  and analysed by XRD to determine the main mineral phases present in the samples (celestine, strontianite, barite, Mg-calcite, dolomite, quartz, kaolinite, illite, and paragonite) and quantify them.

## 2.3. DMC Separation Experiments

To study the separation process of the celestine ore using a dense media, a series of tests were conducted with a dense media hydrocyclone plant.

To prepare the pulp, ferrosilicon (FeSi) (type C40; 82%–90% < 45  $\mu\text{m}$ , particle size; density 7.42 kg/L) was used to prepare a dense medium, as described in detail elsewhere [3]. The density of the dense medium pulp fed into the hydrocyclone was varied

in the 2.7–2.9 kg/L range. To determine the density of the dense medium, the following Equations (1) and (2) were considered:

$$\frac{m_a + m_b + m_c}{V_T} = \rho; \tag{1}$$

$$\frac{m_a}{\rho_a} + \frac{m_b}{\rho_b} + \frac{m_c}{\rho_c} = V_T; \tag{2}$$

where  $m_a$  is the mass of the water,  $m_b$  is the mass of the FeSi,  $m_c$  is the mass of the ore before entering the hydrocyclone,  $\rho$  is the average density of the pulp in the tank, and  $V_T$  is the volume of the tank.

Once the pulp is prepared in the tank, it is then fed tangentially through the feed inlet into the hydrocyclone, entering at a pressure that provides a velocity and centrifugal force that can result in the separation of mineral particles by their different densities. The mineral phases heavier than the cutoff density of the dense medium move towards the wall of the cyclone with a spiral flow and are discharged through the lower orifice called the apex (underflow stream), while the lighter phases float and are discharged through the upper orifice called the vortex (overflow stream). The ferrosilicon is recovered along with the mineral fractions collected in the float and sink sections.

Separation by dense media is based on the difference in density of the mineral phases (Figure 3) and Archimedes’ Principle (Equation (3)) [12].

$$F = V(\rho_x - \rho) \frac{V_t^2}{r} \tag{3}$$

where  $V$  is the volume of the material ( $\text{cm}^3$ ),  $\rho_x$  and  $\rho$  are the density of the material and the suspension ( $\text{g}/\text{cm}^3$ ), respectively,  $V_t$  is the tangential velocity of the material at the rotation radius  $r$  ( $\text{cm}/\text{s}$ ), and  $r$  is the radius of rotation of the material ( $\text{cm}$ ).

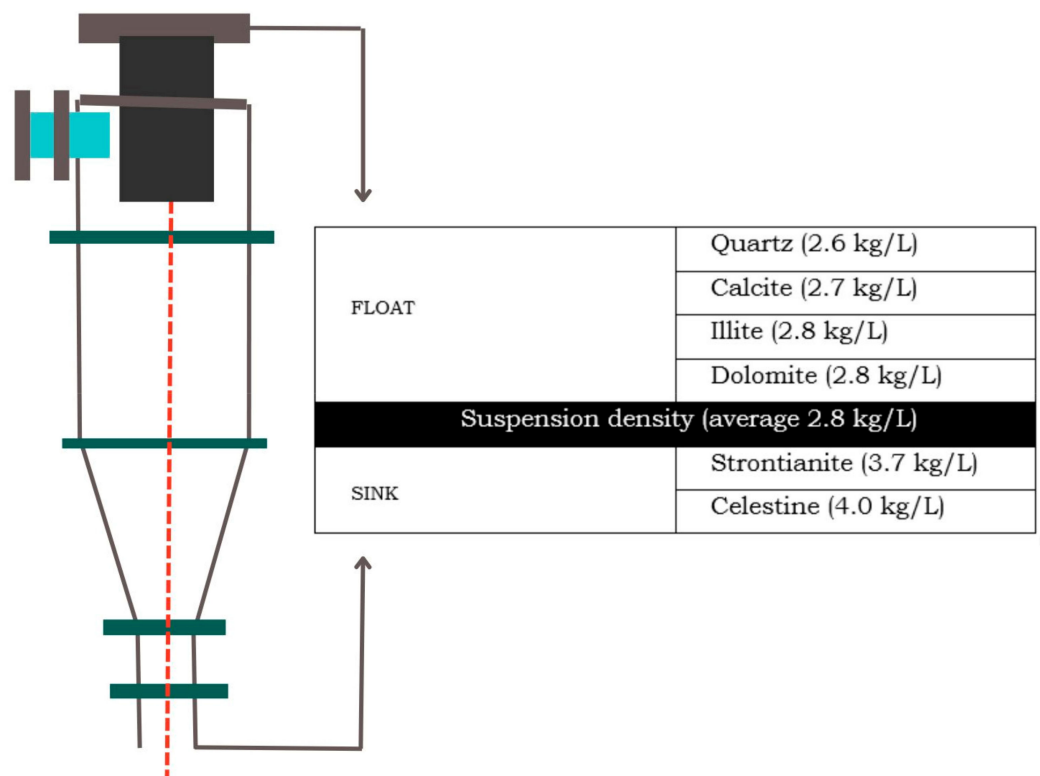


Figure 3. Schedule of phases separation into hydrocyclone.

If  $\rho_x > \rho$ , the value of  $F$  is positive, and the mineral will move outward. Conversely, if  $\rho_x < \rho$ , the value of  $F$  is negative, and the materials will be concentrated in the inner layer.

Three parameters are used to characterise the separation performance: the enrichment ratio ( $E$ , Equation (4)), the tailings discarding ratio ( $R$ , Equation (5)), and the mineral processing recovery ( $\epsilon$ , Equation (6)) [12]:

$$E = \frac{[C]}{[F]} \tag{4}$$

$$R = \frac{M_F - M_C}{M_F} \times 100\% \tag{5}$$

$$\epsilon = \frac{M_C [C]}{M_F [F]} \tag{6}$$

where  $[C]$  is the concentration of concentrated ore (recovered from the sink stream),  $[F]$  is the concentration of the raw ore,  $M_C$  is the mass of concentrated mineral, and  $M_F$  is the mass of the raw ore used as input.

The concentration plant consists of the following parts shown in the layout of Figure 4: a mixing tank (1100 L), a slurry pump, a hydrocyclone, two vibrating screens with sprays, and a magnetic separator.

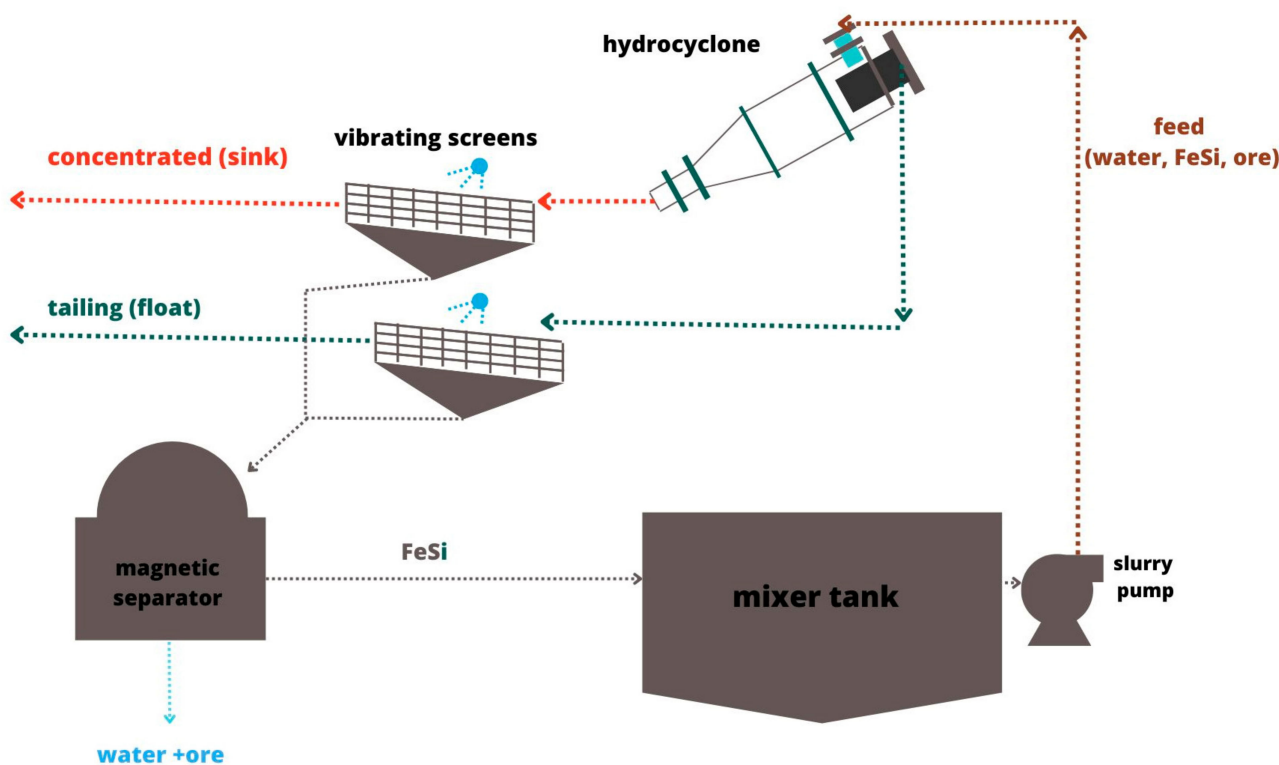


Figure 4. Schedule of pilot plant equipment.

The mixture of water, ferrosilicon (FeSi), and raw ore is fed into the hydrocyclone with a slurry pump. Inside the hydrocyclone, mineral particles are separated by density (see mineral phase distribution). The float stream (with the gangue mineral) is collected by the vortex, and the sink stream (with the concentrate; enriched in celestine) is collected by the apex. The floating and sinking streams go into two vibrating screens (or a single screen with a divider separating the two screens) that collect the mineral, whereas the ferrosilicon (with a fine particle size) and water go through the screen. As there is a certain amount of mineral particles (fines) that remain attached to the FeSi particles, a magnetic separator is used to retain and recirculate the FeSi back to the mixing tank.

The most important parts of the concentration plant are the hydrocyclone (250 mm internal diameter) and the screener, which must maintain the same ratio of design dimensions.

The hydrocyclone was designed according to the following characteristics and design parameters (Figure 5, Table 3). Some parameters were predefined by the structure, and the rest were adjusted to fit the design.

**Table 3.** Hydrocyclone parameters.

Acronym	Parameter	Equation or Value	
Q	Flow rate	$Q = 0.00094 \cdot D_c^2 \cdot P^{0.5}$	[14]
D	Body diameter	250 mm	Predefined
Di	Feed diameter	$Di = \sqrt{4 \frac{bh}{\mu}}$	[15]
Do	Vortex diameter	$\frac{D}{8} \leq Do \leq \frac{D}{5}$	[16]
Du	Apex diameter	$\frac{D}{10} \leq Du \leq \frac{D}{5}$	[17] Bradley Equation
Du/Do	Ratio Du/Do	$0.34 \leq \frac{Du}{Do} \leq 0.9$	[18]
$\theta$	Angle of conical section	20°	Predefined
Hci	Height of cylindrical section	200 mm	Predefined
Hco	Height of conical section	600 mm	Predefined
P	Operating head	Minimum 9D	

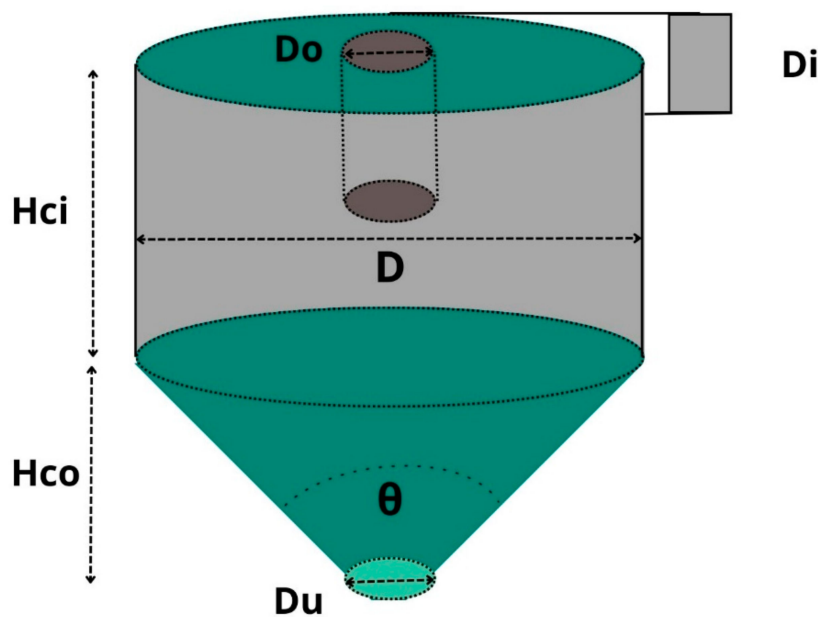


**Figure 5.** Design parameter in a DMS hydrocyclone (created based on (Tórres et al. [16])).

The total surface area of the two screens was calculated using the VSMA method, considering 1 mm rectangular polyurethane mesh (Nuba, modular TS system), and a solids density of 2.9 kg/L. The strainers were also equipped with a motor vibrator of 3 kW power. The calculated theoretical filtration surface was 4.24 m<sup>2</sup> applying a safety factor of 1.4. The equipment with the most suitable dimensions for the calculated filtration surface was a Hein–Lehmann equipment of 4 mm × 1.55 mm.

A horizontal centrifugal slurry pump (type AMP 3/2 B-MAR) was used. It is designed for pumping dense media with heavy-duty hydraulic parts and equipped with a centrifugal seal. The pump has a suction size of 3'' (DN80) and a delivery size of 2'' (DN50). It uses an 18.5 kW 4P IE3 IP55 motor.

To analyse the results of the mineral concentration experiments using the hydrocyclone plant, the response variables to maximise were Sr% or Celestine%, and the continuous and controllable experimental factors were the density inside the hydrocyclone (2.7–2.9 kg/L), the hydrocyclone inclination (15–25), and the hydrocyclone inlet pressure (0.8–1.2 bar). The experimental design was adjusted to a response surface according to the BBD model with centre points [19–21]. The DBB model is used in this study to refine the relevant experimental parameters of the mineral concentration process that need to be optimised. For the model, equally distributed values of each parameter were used. Statgraphics Centurion XVI software (version 16.1.03) was used to calculate and plot the response surface.

### 3. Results and Discussion

#### 3.1. Characteristics of Celestine Ore Sample

The mineralogical composition of the raw mineral after the desliming process is summarised in Table 4. This analysis shows that the main mineral phases present in the sample are celestine, strontianite, dolomite, calcite, and illite. Additionally, the mineral fractions with the largest particle size (>3.15 mm) have the highest content of celestine (over 84%) and constitute 55.56% of the total mass of the sample. On the other hand, the mineral fraction with the smallest particle sizes (the fines; <1 mm) has the lowest celestine concentration (74.81%) and represents 15% of the total mass of the sample.

**Table 4.** Mineral concentration in the raw celestine ore sample determined by XRD for the different particle size fractions.

		Celestine %	Strontianite %	Quartz %	Dolomite %	Calcite %	Illite %
<b>Raw fraction</b>	100.00	83.33	0.4	3.39	2.54	9.79	0.55
<b>&gt;5 mm</b>	30.55	84.10	0.21	3.36	3.15	8.68	0.51
<b>(−5 mm + 3.15 mm)</b>	25.01	83.04	0.14	2.75	3.14	7.53	0.41
<b>(−3.15 mm + 2 mm)</b>	15.25	80.99	0.30	2.41	3.93	11.96	0.41
<b>(−2 mm + 1 mm)</b>	14.10	80.42	0.34	3.39	3.16	12.20	0.45
<b>&lt;1 mm</b>	15.09	74.81	0.69	9.04	2.29	12.41	0.76

The greater particle size fractions (>5 mm) have the highest content of celestine (over 84%) and constitute 30.55% of the total mass sample. The fines (<1 mm) have a lower celestine concentration (74.81%) and represent 15% of the total sample.

#### 3.2. Evaluation of Gravity Separation

##### 3.2.1. Particle Size Tests

To study the range of densities suitable for separation into the hydrocyclone system, SPT-1 was applied to each of the granulometric fractions above 1 mm. Mineral fractions below 1 mm could not be studied due to the difficulty of performing the technique with such fine particle size. Once the tests were performed, the flotation and sinking products were analysed by XRD (Table 5).

Table 6 shows data on the mass % of the different mineral phases present in the mineral collected in floated and sunk products. The increase in the concentration of celestine in the sunk product translates into an increase in the concentration of calcite in the floated product.

For the dense medium with a density of 2.7 kg/L, the increase between the concentration of celestine in the sunk phase and the feed, as well as the low mass recovered in the flotation, show that no mineral separation has been achieved.

For the dense medium with a density of 2.8 kg/L, there is a higher increase in the concentration of celestine mineral (>5 mm = 7.83%; −5 mm + 3.15 mm = 7.51%; −3.15 mm + 2 mm = 9.97%; −2 mm + 1 mm = 4.69%) than in the case of a dense medium of 2.9 kg/L.

We also observed that there is also an increase in the quartz concentration in the floated product for particle size fractions greater than 2 mm.

**Table 5.** XRD analysis of mineral samples collected from the float–sink streams.

Density (Kg/L)	Size Fraction	Yield (%)	Products	Recovery Mass (g)	Celestine %	Trontianite %	Quartz %	Dolomite %	Calcite %	Illite %
2.7	(-6 mm + 5 mm)	30.55	Floats	1.87	10.25	0.17	3.00	41.72	43.72	1.14
			Sink	98.13	85.51	0.33	2.16	1.70	9.84	0.47
			Feed	100.00						
	(-5 mm + 3.15 mm)	25.01	Floats	1.78	4.86	0.18	3.69	59.69	30.52	1.06
			Sink	98.22	84.46	0.04	2.75	2.12	10.22	0.42
			Feed	100.00						
	(-3.15 mm + 2 mm)	15.25	Floats	2.95	4.07	0.77	7.94	35.68	50.73	0.79
			Sink	97.05	83.33	0.27	1.60	1.97	12.31	0.52
			Feed	100.00						
	(-2 mm + 1 mm)	14.10	Floats	4.19	3.98	0.54	4.30	32.67	54.41	1.10
			Sink	95.81	83.76	0.06	1.87	1.90	11.91	0.49
			Feed	100.00						
2.8	(-6 mm + 5 mm)	30.55	Floats	11.88	26.01	0.61	5.12	1.21	67.01	0.04
			Sink	88.12	91.93	0.22	1.83	0.41	5.12	0.50
			Feed	100.00						
	(-5 mm + 3.15 mm)	25.01	Floats	12.36	29.80	1.05	5.33	2.76	58.93	2.13
			Sink	87.64	90.55	0.01	3.45	0.43	4.79	0.77
			Feed	100.00						
	(-3.15 mm + 2 mm)	15.25	Floats	13.81	18.77	0.59	12.84	0.71	65.95	1.15
			Sink	86.19	90.96	0.03	3.51	0.48	4.45	0.57
			Feed	100.00						
	(-2 mm + 1 mm)	14.10	Floats	6.95	17.61	0.23	1.70	22.89	56.05	1.52
			Sink	93.05	85.11	0.27	5.54	0.05	9.04	0.00
			Feed	100.00						
2.9	(-6 mm + 5 mm)	30.55	Floats	16.24	48.68	2.11	5.52	0.64	41.24	1.80
			Sink	83.76	90.97	0.45	1.92	0.55	5.48	0.64
			Feed	100.00						
	(-5 mm + 3.15 mm)	25.01	Floats	4.54	41.65	2.08	8.93	0.83	44.98	1.51
			Sink	95.46	85.01	0.39	2.93	0.50	10.48	0.69
			Feed	100.00						
	(-3.15 mm + 2 mm)	15.25	Floats	5.85	37.02	2.03	4.55	0.88	54.23	1.29
			Sink	94.15	83.72	0.10	5.25	1.55	9.00	0.38
			Feed	100.00						
	(-2 mm + 1 mm)	14.10	Floats	16.85	36.81	2.15	3.58	0.90	55.99	0.57
			Sink	83.15	89.26	0.54	1.18	0.61	8.19	0.23
			Feed	100.00						

**Table 6.** Parameters to describe the separation performance of the DSM experiments.

Density (Kg/L)	Size Fraction	$\epsilon$	E	R
2.7	>5 mm	99.77	1.02	1.87
	(−5 mm + 3.15 mm)	99.90	1.02	1.78
	(−3.15 mm + 2 mm)	99.85	1.03	2.95
	(−2 mm + 1 mm)	99.79	1.04	4.19
2.8	>5 mm	96.33	1.09	11.88
	(−5 mm + 3.15 mm)	95.56	1.09	12.36
	(−3.15 mm + 2 mm)	96.80	1.12	13.81
	(−2 mm + 1 mm)	98.48	1.06	6.95
2.9	>5 mm	90.60	1.08	16.24
	(−5 mm + 3.15 mm)	97.72	1.02	4.54
	(−3.15 mm + 2 mm)	97.33	1.03	5.85
	(−2 mm + 1 mm)	92.29	1.11	16.85

### 3.2.2. Separation Density Tests

From the separation density tests, the main parameters describing the process performance ( $\epsilon$ , E, and R) were determined from the product mass data and the percentages of celestine recovered in the float and sink products starting from the different mineral fractions with different particle sizes (see Table 6).

For a dense medium with density of 2.7 kg/L, the enrichment rate was rather low (E = 1.023; 2.3%), detecting little variation with mineral particle size.

For a dense medium with a density of 2.8 kg/L, there is a higher enrichment rate of E = 1.092 (9.2%) and, as expected, a higher recovery rate.

On the other hand, for an even higher density of the medium (2.9 kg/L), the enrichment rate decreases notably (E = 1.061; 6.1%). These results do not follow the trend of increasing enriching with the density of the media observed by other authors [12]. Thus, in this case, the best results were obtained at a density 2.8 kg/L. The poorer results obtained at higher densities, at 2.9 kg/L (near the saturation point), could be due to the high viscosity that greatly increases decanting times and may cause species identification problems due to the recrystallisation of SPT-1, which causes difficulties in removal. [22,23]. In addition, higher density solutions are more sensitive to water evaporation, which will cause a significant change in density and may cause the solution (SPT) to become more viscous and cause SPT crystallisation [24,25].

### 3.3. Separation Performance of DMS

To study the behaviour of the hydrocyclone DSM system, a series of experiments were defined to study the mineral fractions: −6 mm + 1 mm (Table S1). A factorial design with 12 experiments and three additional central points (15 experiments in total) was used to test the influence of three controllable factors (pulp density, inclination, and inlet pressure) and three response levels. Table S1 contains the number of experiments required for the three-parameter, three-level spaced DBB model designed. For this study, the factors or experimental parameters considered were the pulp density (level 2.7 kg/L–level 2.8 kg/L–level 2.9 kg/L), hydrocyclone inclination with respect to the horizontal plane (level 15.00°–level 20.00°–level 25°), and inlet pressure (0.8 Bar–1.00 Bar–1.2 Bar). Fifteen tests were performed, and the results were analysed using the software Statgraphics Centurion. The optimum values of parameters that maximise both Sr concentration (determined by XRF) and celestine concentration (determined by XRD) in the under stream were estimated.

Representative mineral samples were collected from the float and sink of the DMS hydrocyclone at the drainer discharge. Then, after drying and grinding the mineral samples (<61 µm), they were analysed by XRF (Sr%, Ca%) and XRD (celestine/calcite).

Note that mineral samples could not be recovered from the under and over streams in experiments using a dense medium of 2.9 kg/L because the sludge pump could not operate at this high density, probably due to the high content of solids in the slurry.

From the chemical and mineralogical composition data of mineral samples collected from the under stream streams in the hydrocyclone tests, regression equations and response surfaces were calculated, and the optimum operating values of parameters were estimated.

In order to produce celestine concentrates using a hydrocyclone, the mathematical model equations were derived from a computer simulation using a least-squares method [26]. The model is obtained relating the concentration of Sr/Celestine of the under stream (as a dependent variable) to the design parameters and their interactions [Equations (7) and (8)].

The statistical and correlation analysis of different input parameters on the response were studied by the analysis of variance [Table 7] [27,28]. Figure S3 shows how the inclination or inlet pressure parameters have a low influence on the Sr or celestine concentration.

**Table 7.** Statistical results of the least-squares method of Sr and celestine concentrations based on the BBD model.

Statistical Parameter	XRD Results	XRF Results
R-squared	99.92%	99.92%
R-squared (adjusted for g.l.)	99.79%	99.78%
Standard error	1.70	1.26
Mean absolute error	0.84	0.64

According to the XRF data, the following model describing Sr concentration was determined:

$$[\text{Sr}] = -25,339.9 + 18,392.6 \times \text{Density} + 1.34983 \times \text{Inclination} + 56.2542 \times \text{Pressure} - 3335.46 \times \text{Density}^2 + 0.215 \times \text{Density} \times \text{Inclination} + 3.875 \times \text{Density} \times \text{Pressure} - 0.0487833 \times \text{Inclination}^2 - 0.1525 \times \text{Inclination} \times \text{Pressure} - 30.4896 \times \text{Pressure}^2 \quad (7)$$

According to the XRD data, the following model describing celestine concentration was determined:

$$[\text{Celestine}] = -35,067.7 + 25,418.8 \times \text{Density} + 3.38692 \times \text{Inclination} + 132.708 \times \text{Pressure} - 4607.42 \times \text{Density}^2 + 0.08 \times \text{Density} \times \text{Inclination} - 2.375 \times \text{Density} \times \text{Pressure} - 0.0629667 \times \text{Inclination}^2 - 0.9475 \times \text{Inclination} \times \text{Pressure} - 50.7917 \times \text{Pressure}^2 \quad (8)$$

On the other hand, the following regression equation can be defined, relating the design parameters (density, inclination, and pressure) to the concentration of Sr/Celestine in the mineral recovered in the under stream [Equations (9) and (10)].

According to the XRF data:

$$[\text{Sr}] = 821.14 - 277.83 \times \text{Density} - 0.15 \times \text{Inclination} + 3.08 \times \text{Pressure} \quad (9)$$

According to the XRD data:

$$[\text{Celestine}] = 1125.0 - 383.46 \times \text{Density} + 0.14 \times \text{Inclination} + 5.52 \times \text{Pressure} \quad (10)$$

The DBB model optimisation helped determine a combination of variables that mutually optimised responses [29,30]. The response surfaces (Figure 6) obtained from the BBD model allowed the calculation of the optimum values of each parameter tested and their interaction effects [27]. To facilitate the visualisation of the model results, Figure 6

represents the influence of two parameters when the third is set at the intermediate level. The points circled in each image (A–F) correspond to the optimum value obtained for each factor. As can be seen in presented panels, the surfaces obtained by XRF (D, E, F) show higher variation in the factors’ studied intervals (greatest difference between the areas where the combination of parameters optimise the response variable).

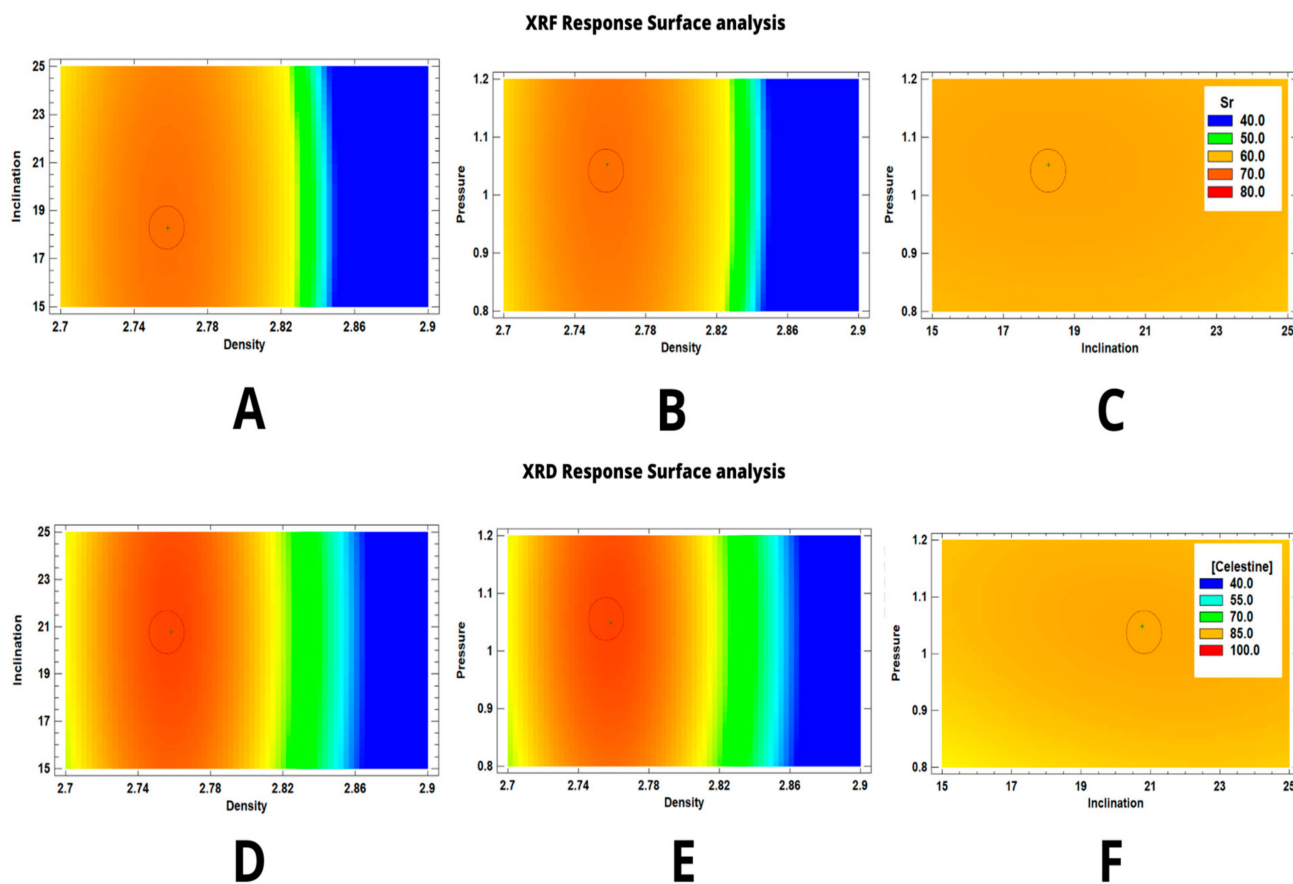


**Figure 6.** DBB model response surfaces. (A) XRF response surface at 1.00 bar inlet pressure. (B) XRF Response Surface at 20.00 inclination. (C) XRF response surface at density 2.8 kg/L. (D) XRD response surface at 1.00 bar inlet pressure. (E) XRD response surface at 20.00 inclination. (F) XRD response surface at density 2.8 kg/L. The points circled in each image (A–F) correspond to the optimum value obtained for each factor.

As main results, the model allows for the identification of optimising values of density, inclination, and pressure to maximise the concentration of Sr (identified by XRF) and Celestine (identified by XRD), as reported in Table 8.

**Table 8.** Optimised values of the factors to obtain maximum values of [Sr] or [Celestine] concentration.

	Factor	Optimum (XRF)	Optimum (DRX)
Factors	Density	2.75	2.75
	Inclination	18.27	20.76
	Pressure	1.05	1.05
Response variable (to be maximised)	[Sr]/[Celestine]	68.4	94.4

### 3.3.1. Effect of Separation Density

The density value inside the DMC hydrocyclone was calculated from density data measured at the apex, vortex, and mixing tank (Table S2).

Density values inside the tank ( $D_{\text{tank}}$ ) above 2.10 kg/L could not be piloted, since it produced blockage problems inside the hydrocyclone system.

With the data obtained from the densities obtained in each vortex and apex test, the average density inside the hydrocyclone system ( $D_{\text{hydrocyclone}}$ ) was calculated from the density of the tank ( $D_{\text{tank}}$ ) using a linear regression model ( $D_{\text{hydrocyclone}} = 1.15 D_{\text{tank}} + 0.45$ ,  $R^2 = 0.96$ ; Figure 7).

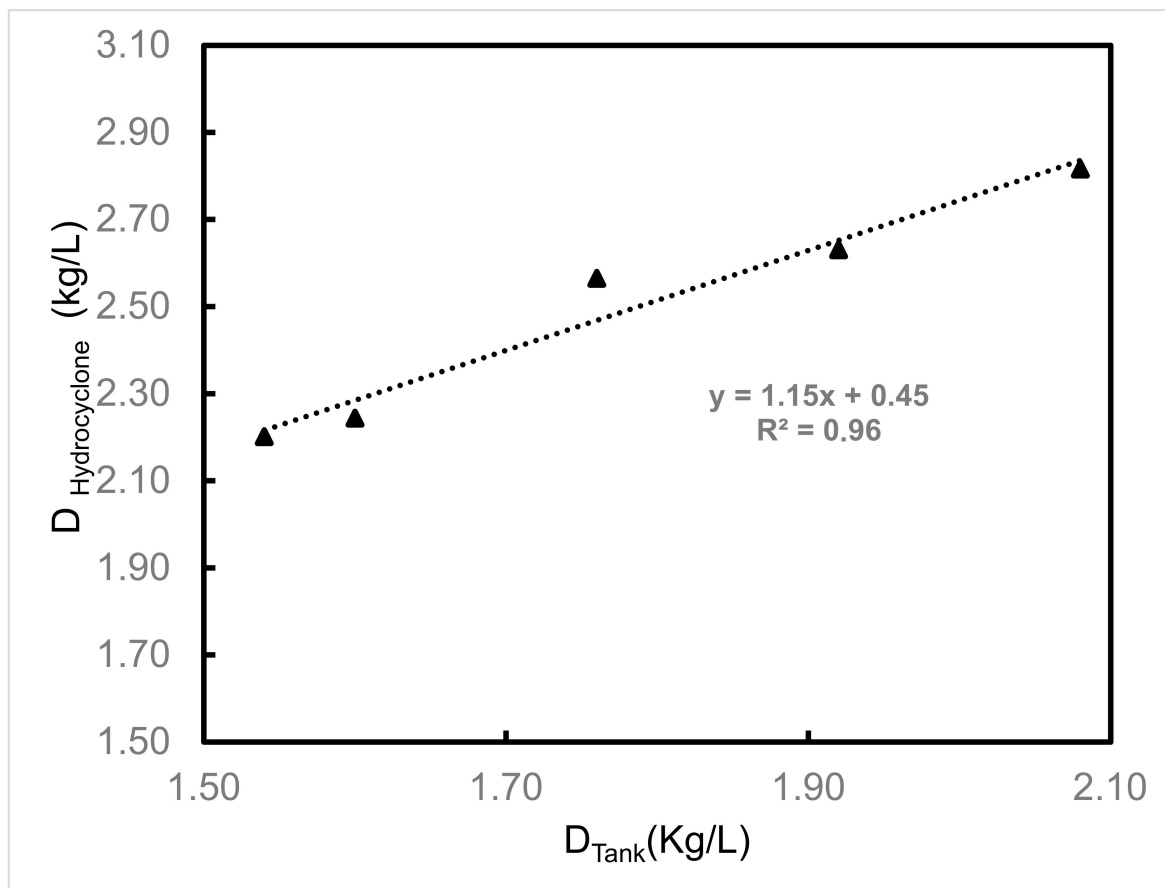


**Figure 7.** Density in the hydrocyclone  $D_{\text{hydrocyclone}}$  as a function of the density in the tank  $D_{\text{Tank}}$ .

The hydrocyclone was designed for mineral separation using the difference in mineral densities, so the effect of dense medium density is the parameter that has the most important contribution to the performance of the separation process, as shown by other authors [28].

According to [31] when the dense medium has a small particle size, a higher separation efficiency and a smaller displacement of the shear point is achieved (providing stability to the medium), although the effects of rheology are more pronounced (having negative effects on the separation efficiency at high densities). On the other hand, if the dense medium is thicker, the rheological effect is not so important, and stability plays an important role, and at high medium densities, better separation results are achieved.

The variable density of 2.7–2.9 kg/L should be that inside the hydrocyclone. The density inside the hydrocyclone is between the densities at the vortex outlet and the apex [12].

For the tests carried out at the density of 2.7 kg/L, an increase in the mass percentage and a poor enrichment in [Ca]/[Calcite] of the overflow stream (except at the conditions of 25° inclination and 1 bar inlet pressure) is observed.

On the other hand, when working at a 2.8 kg/L density, a mass % of the underflow higher than 74.48% was obtained with grades higher than 61% Sr and 71% [Celestine] at pressures higher than 1 bar, with [Ca]/[Calcite]% below the inlet values (Table S1). An optimum hydrocyclone media density of 2.76 kg/L (obtained in both XRF and XRD analytical techniques) has been calculated for which the Sr/Celestine concentration in the under stream is maximised (Table 8).

### 3.3.2. Effect of Inlet Pressure

In the cyclone body, the suspension is pushed towards the wall, decreasing the static pressure from the wall towards the centre [32] creating a pressure gradient in the radial direction. Thus, if the force derived from the pressure gradient is greater than the centrifugal force, the particle will float, being a product of the vortex. In the opposite case, the particle will be a product of the apex [33]. An increase in the inlet pressure has increased the static pressure gradient along the radius, increasing vortex products [32].

The application of high-inlet pressure in a dense-medium cyclone to provide high centrifugal force has recently been shown to allow for efficient separation for the treatment of fines. Although high pressure requires specialised pumps [33,34] and can produce ore grinding due to ore crushing inside the pump.

Inlet pressure (along with geometric dimensions) influences hydrocyclone performance through the split ratio (the ratio of hydrocyclone underflow volumetric flow rate to feed volumetric flow rate) [35].

For the tests carried out at the inlet pressure of 0.8 bar, a low enrichment of the under stream in [Sr]/[Celestine] is observed, while high pressures of 1.2 bar did not yield the best concentration results either (Table S1). An optimum hydrocyclone inlet pressure of 1.05 bar (obtained in both XRF and XRD analytical techniques) has been calculated for which the Sr/Celestine concentration in the under stream is maximised (Table 8).

### 3.3.3. Effect of Inclination

According to [36], a slope greater than 45° has a significant effect on the performance of high diameter, low-pressure hydrocyclones. As the inclination increases, the shear point and water recovery increase [28].

In addition, the effect of inclination is significant at solids percentages greater than 10% [37]. Lower inclination angles, measured from the horizontal, facilitate the exit of coarse and higher density mineral particles in the over stream. From the horizontal plane, the greater inclination of the hydrocyclone will make a less coarse and less dense cut [38].

An optimum inclination rate grade of 18°–20° (obtained in both XRF and XRD analytical techniques) has been calculated for which the Sr/Celestine concentration in the under stream is maximised (Table 8).

## 4. Conclusions

In this study, a factorial experimental design has been used to optimise the operating parameters of a dense media hydrocyclone system (applicable to a range of hydrocyclones with the characteristics included in Table 3), with the main objective of concentrating the celestine mineral (of medium grade 60%–80% celestine) from the Montevive mine.

Considering the mineral composition data determined by XRD, from mineral fractions with different particle size, fractions with particle size greater than 5 mm, which account for more than 30% by mass of the sample, have an average grade of 84.10% celestine.

In the sink–float mineral–dense medium experiments at laboratory scale to study the optimum density inside the hydrocyclone, it was seen that the mineral phases that sank are celestine and strontianite, and the mineral phases that floated are quartz, dolomite, calcite, and illite. Better phase separation results were obtained with the intermediate density of 2.8 kg/L, which produced the highest recovery and enrichment values.

Validation tests in the hydrocyclone showed that the optimum value to maximise [Sr]/[Celestine] with dense medium densities was 2.75 kg/L, at an inlet pressure of 1.05 bar and inclinations of 18°–20°, achieving a 94% recovery of celestine (68% Sr).

These preliminary results serve as a starting point for future studies to validate the effectiveness of this treatment methodology under industrial conditions and to assess its economic and environmental feasibility on a large scale.

**Supplementary Materials:** The following supporting information can be downloaded at: <https://www.mdpi.com/article/10.3390/min14030306/s1>, Figure S1: Elemental analysis by XRF of validation samples, Figure S2: DRX diagram of validation sample, Table S1: Test design to validate results in hydrocyclone system, Figure S3: Main effects of Sr/Celestine optimization (A) by XRF (B) by DRX, Table S2: Density inside hydrocyclone tests.

**Author Contributions:** Conceptualization and methodology: A.B.R.-N., M.J.M.-B., M.C.d.H. and N.A.-R.; software, N.A.-R. and M.J.M.-B.; validation and formal analysis: A.B.R.-N., N.A.-R. and F.O.; investigation: A.B.R.-N., N.A.-R. and F.O.; writing—original draft preparation, A.B.R.-N., M.J.M.-B. and N.A.-R.; writing—review and editing: A.B.R.-N., M.J.M.-B., N.A.-R. and M.C.d.H.; project administration and funding acquisition: A.B.R.-N. and M.J.M.-B. All authors have read and agreed to the published version of the manuscript.

**Funding:** This research was funded by ROTATE PROJECT 101058651 (European Union).

**Data Availability Statement:** All data are freely available and can be requested from the authors.

**Acknowledgments:** We thank Gordon Parkin for his supervision and review of results and conclusions.

**Conflicts of Interest:** Author Alejandro B. Rodríguez-Navarro, was employed by the Canteras Industriales S.L. Company. The remaining authors declare that the research was conducted in the absence of any commercial or financial relationships that could be construed as a potential conflict of interest.

## References

1. Jimeno, C.L.; González, C.M. Las materias primas minerales y la transición energética. *Cuad. Estrateg.* **2022**, *209*, 61–174.
2. Jiménez-Peñalvarez, J.D. Nieve, Oro, Sal, Estroncio. Historia de la Minería en Granada. 2008. Available online: <https://www.ugr.es> (accessed on 17 September 2023).
3. Ariza-Rodríguez, N.; Rodríguez-Navarro, A.B.; de Hoces, M.C.; Muñoz-Batista, M.J. Laboratory-Scale Optimization of Celestine Concentration Using a Hydrocyclone System. *Appl. Sci.* **2023**, *13*, 10206. [CrossRef]
4. Luukkanen, S.; Tanhua, A.; Zhang, Z.; Mollehuara Canales, R.; Auranen, I. Towards waterless operations from mine to mill. *Miner. Eng.* **2022**, *187*, 107793. [CrossRef]
5. Sulman, H.L.; Picard, H.F.K.; Ballot, J. Ore Concentration. 835 120, 6 November 1906. Available online: <https://patentimages.storage.googleapis.com/31/20/dc/39d20dc025985d/US835120.pdf> (accessed on 10 September 2023).
6. Wills, B.A. *Tecnología de Procesamiento de Minerías: Tratamiento de Menas y Recuperación de Minerales*; Limusa: Mexico City, Mexico, 1987; Volume 517.
7. Ballester, A.; Verdejo, L.F.; Sancho, J. *Metalurgia Extractiva*; Síntesis: Madrid, Spain, 2014; Volume 1.
8. Gálvez Borrego, A. Agentes de Superficie Aniónicos en la Flotación de Celestina y Calcita. Ph.D. Thesis, Universidad de Granada, Granada, Spain, 1993.
9. Corpas-Martínez, J.R. Concentración de Minerales Mediante Métodos Físico-Químicos. Aplicación a la Obtención de Fluorita de Alta Pureza. 2021. Available online: <http://hdl.handle.net/10481/66396> (accessed on 5 December 2023).
10. Feng, Q.; Yang, W.; Chang, M.; Wen, S.; Liu, D.; Han, G. Advances in depressants for flotation separation of cu-fe sulfide minerals at low alkalinity: A critical review. *Int. J. Miner. Metall. Mater.* **2024**, *31*, 1–17. [CrossRef]
11. Ariza-Rodríguez, N.; Rodríguez-Navarro, A.B.; Calero de Hoces, M.; Martín, J.M.; Muñoz-Batista, M.J. Chemical and Mineralogical Characterization of Montevive Celestine Mineral. *Minerals* **2022**, *12*, 1261. [CrossRef]
12. Lv, Z.; Wei, M.; Zhao, D.; Wu, D.; Liu, C.; Cheng, H. Preconcentration of a low-grade betafite ore by dense medium cyclone. *Physicochem. Probl. Miner. Process.* **2022**, *58*, 143338. [CrossRef]
13. Sobhy, A. Recent Trends in Mineral Processing Based on Density and Particle Size—A review. *Int. J. Mater. Technol. Innov.* **2022**, *2*, 13–30. [CrossRef]
14. Mular, A.L.; Jull, N.A. Classification. In *Mineral Processing Plant Design*; Mular, A.L., Bhappu, R.B., Eds.; Elsevier B. V.: Amsterdam, The Netherlands, 2006; Chapter 17; p. 385.
15. Sanchez, Z.; Emilio, L.E. *Operaciones Unitarias en Preparación de Minerales*; Universidad Nacional, Facultad de Minas: Medellín, Columbia, 1988.

16. Tórres, I.D.A.; Molina, C.A.S.; Tascón, C.E.O. Parámetros de diseño de un hidrociclón para clasificar café pergamino. *Rev. Fac. Nac. Agron. Medellín* **1998**, *51*, 191–215.
17. Lodoño, R.G.E.; Pérez, G.J.E. *Hidrociclones: Alternativa en la Separación Sólido Líquido*; Universidad Pontificia Bolivariana, Facultad de Ingeniería: Medellín, Columbia, 1988; 253p.
18. Bustamante, M.O. Efecto de la Geometría de un Hidrociclón Sobre las Condiciones Normales de Operación. Master's Thesis, Universidad de Concepción, Concepcion, Chile, 1989.
19. Box, G.E.P.; Behnken, D.W. Some new three level designs for the study of quantitative variables. *Technometrics* **1960**, *2*, 455–475. [[CrossRef](#)]
20. Dixit, P.; Tiwari, R.; Mukherjee, A.K.; Banerjee, P.K. Application of response surface methodology for modeling and optimization of spiral separator for processing of iron ore slime. *Powder Technol.* **2015**, *275*, 105–112. [[CrossRef](#)]
21. Özgen, S.; Yildiz, A. Application of Box–Behnken design to modeling the effect of smectite content on swelling to hydrocyclone processing of bentonites with various geologic properties. *Clays Clay Miner.* **2010**, *58*, 431–448. [[CrossRef](#)]
22. Krukowski, S.T. Sodium metatungstate: A new heavy-mineral separation medium for the extraction of conodonts from insoluble residues. *J. Paleontol.* **1988**, *62*, 314–316. [[CrossRef](#)]
23. Mazarío, F.P.; Martínez, R.R.; Costa, S.H. Mejoras en la separación de minerales pesados usando politungstato sódico. *Geogaceta* **1991**, *11*, 54–56.
24. Savage, N.M. The use of sodium polytungstate for conodont separations. *J. Micropalaeontol.* **1988**, *7*, 39–40. [[CrossRef](#)]
25. Skipp, G.; Brownfield, I.K. *Improved Density Gradient Separation Techniques Using Sodium Polytungstate and a Comparison to the Use of Other Heavy Liquids*; US Department of the Interior, US Geological Survey: Denver, CO, USA, 1993.
26. Ozgen, S.; Yildiz, A.; Çalıskan, A.; Sabah, E. Modeling and optimization of hydrocyclone processing of low grade bentonites. *Appl. Clay Sci.* **2009**, *46*, 305–313. [[CrossRef](#)]
27. Bhandary, A.; Mukherjee, S.; Rajib, D.; Ghosh Chaudhuri, M. Mineralogical studies and optimization of tabling parameters of low grade chromite ore by box behnken design of experiments. *J. Met. Mater. Miner.* **2022**, *32*, 174–185. [[CrossRef](#)]
28. Vakamalla, T.; Narasimha, M. Rheology-based CFD modeling of magnetite medium segregation in a dense medium cyclone. *Powder Technol.* **2015**, *277*, 275–286. [[CrossRef](#)]
29. Arroug, L.; Elaatmani, M.; Zegzouti, A. A preliminary study to investigate the beneficiation of low-grade phosphate sludge using reverse flotation: Modeling and optimization through box-behnken design and response surface methodology. *Chem. Eng. Res. Des.* **2024**, *204*, 228–237. [[CrossRef](#)]
30. Huo, Q.; Liu, X.; Chen, L.; Wu, Y.; Wu, H.; Xie, J.; Liu, X.-X.; Qiu, G. Treatment of backwater in bauxite flotation plant and optimization by using box-behnken design. *Trans. Nonferrous Met. Soc. China* **2019**, *29*, 821–830. [[CrossRef](#)]
31. He, Y.B.; Laskowski, J.S. Effect of dense medium properties on the separation performance of a dense medium cyclone. *Miner. Eng.* **1994**, *7*, 209–221. [[CrossRef](#)]
32. Bhaskar, K.U.; Murthy, Y.R.; Raju, M.R.; Tiwari, S.; Srivastava, J.K.; Ramakrishnan, N. CFD simulation and experimental validation studies on hydrocyclone. *Miner. Eng.* **2007**, *20*, 60–71. [[CrossRef](#)]
33. Wang, B.; Chu, K.W.; Yu, A.B.; Vince, A. Modeling the Multiphase Flow in a Dense Medium Cyclone. *Ind. Eng. Chem. Res.* **2009**, *48*, 3628–3639. [[CrossRef](#)]
34. Suresh, P.D.; Kumar, V.; Sripriya, R.; Chakraborty, S.; Meikap, B.C. Performance characteristics of pilot plant dense media hydrocyclone for beneficiation of coal and 3-D CFD simulation. *Chem. Eng. Sci.* **2010**, *65*, 4661–4671. [[CrossRef](#)]
35. He, Y.B.; Laskowski, J.S. Dense Medium Cyclone Separation of Fine Particles Part 1. The Effect of Medium Split Ratio on Dense Medium Cyclone Performance. *Coal Prep.* **1995**, *16*, 1–25. [[CrossRef](#)]
36. Asomah, A.K.; Napier-Munn, T.J. An empirical model of hydrocyclones incorporating angle of cyclone inclination. *Miner. Eng.* **1997**, *10*, 339–347. [[CrossRef](#)]
37. Banisi, S.; Deghan-Nayeri, H. Effect of angle of hydrocyclone inclination on cut size. *Can. Metall. Q.* **2005**, *44*, 79–84. [[CrossRef](#)]
38. McLanahan. Los 5 Aspectos Que Deber Saber Sobre los Hidrociclones. 29 April 2019. Available online: <https://www.mclanahan.com/es/blog/los-5-aspectos-que-deber-saber-sobre-los-hidrociclones> (accessed on 27 November 2023).

**Disclaimer/Publisher's Note:** The statements, opinions and data contained in all publications are solely those of the individual author(s) and contributor(s) and not of MDPI and/or the editor(s). MDPI and/or the editor(s) disclaim responsibility for any injury to people or property resulting from any ideas, methods, instructions or products referred to in the content.